JOURNAL OF GUIDANCE, CONTROL, AND DYNAMICS
Vol. 42, No. 2, February 2019

Semianalytical Technique for Six-Degree-of-Freedom Space Object Propagation

Noble Hatten* and Ryan P. Russell†
The University of Texas at Austin, Austin, Texas 78712-1221

DOI: 10.2514/1.G003706

The cannonball assumption of three-degree-of-freedom (3DOF) space object state prediction can lead to large inaccuracies if the sphericity assumption is violated, while numerical propagation of both the translational and rotational (6DOF) equations of motion is computationally expensive. In this paper, a middle ground is proposed, in which the translational equations of motion are propagated numerically using approximate attitude predictions obtained via a closed-form perturbation solution. The capabilities of this semianalytical "hybrid" of special and general perturbation techniques are illustrated using a specific attitude solution, which assumes a fast-rotating, triaxial rigid body in an elliptical orbit subject to gravity-gradient torque. Even when these assumptions are mildly violated—such as when modeling higher-fidelity forces and torques—the approximate attitude predictions allow for more accurate modeling of body forces than a 3DOF cannonball propagation. In numerical examples in which attitude-dependent dynamics are considered, the hybrid method produces position predictions one or more orders of magnitude more accurate than a 3DOF cannonball propagation while requiring approximately one-third of the CPU time of a full 6DOF propagation for certain accuracy tolerance levels. Relative speedups achievable by the hybrid method are shown to increase as the rotation rate of the body increases.

Nomenclature

A, B, C	=	principal moments of inertia such that $A \leq B \leq C$ ($\text{kg} \cdot \text{m}^2$ unless otherwise noted)
a	=	semimajor axis (km unless otherwise noted)
$\dot{a}$	=	time derivative of arbitrary variable a
e	=	eccentricity
f	=	as subscript: final
$\boldsymbol{f}$	=	state equation vector (i.e., time derivative of state vector)
i	=	inclination (deg unless otherwise noted); as subscript: index variable
J_i	=	ith-order zonal gravitational potential coefficient
Q	=	closed-form attitude solver reinitialization criteria
$\bar{\boldsymbol{q}}$	=	quaternion, organized such that q_4 is the scalar element
$\boldsymbol{r}$	=	position vector of space object in Earth-centered inertial reference frame (km unless otherwise noted)
rot	=	as subscript: rotational
t	=	time (seconds unless otherwise noted)
tr	=	as subscript: translational
x, y, z	=	as subscripts: components of a three-dimensional vector
$\boldsymbol{x}$	=	state vector
ϵ	=	small parameter of a perturbation method
ν	=	true anomaly (deg unless otherwise noted)
Ω	=	right ascension of the ascending node (deg unless otherwise noted)
ω	=	argument of periapsis (deg unless otherwise noted)
$\boldsymbol{\omega}$	=	angular velocity vector (deg/s unless otherwise noted)
$\boldsymbol{\xi}$	=	Lara-Ferrer attitude perturbation solution variable set
$\boldsymbol{\xi}'$	=	singly averaged Lara-Ferrer attitude perturbation solution variable set
$\boldsymbol{\xi}''$	=	doubly averaged Lara-Ferrer attitude perturbation solution variable set
ϕ, θ, ψ	=	precession (deg), nutation (deg), and spin (deg), respectively; a 3-1-3 Euler angle sequence
0	=	as subscript: initial
1, 2, 3, 4	=	as subscripts: quaternion elements, such that elements {1,2,3} make up the vector portion

Received 17 March 2018; revision received 21 July 2018; accepted for publication 12 August 2018; published online 9 November 2018.

*Research Associate, Department of Aerospace Engineering and Engineering Mechanics, 210 E. 24th St. Stop C0600; noble.hatten@gmail.com. Student Member AIAA.

†Associate Professor, Department of Aerospace Engineering and Engineering Mechanics, 210 E. 24th St. Stop C0600; ryan.russell@utexas.edu. Associate Fellow AIAA.

I. Introduction

THERE is no closed-form solution for the evolution of the state of a space object (SO) under the influence of the full range of forces (and torques) to which SOs are subject. Consequently, many methods of approximation have been developed, which may be broadly classified into three groups: numerical methods (i.e., special perturbations), analytical methods (i.e., general perturbations), and semianalytical methods [1]. All three classes see widespread use due to the classic relationship between model fidelity and computational efficiency: Increasing the accuracy of a prediction generally necessitates a corresponding increase in compute time.

On one end of the spectrum, special perturbation (SP) methods use numerical techniques (e.g., Runge–Kutta) to propagate an approximation of the solution of a system of ordinary differential equations (ODEs), step by step, from initial conditions to the time of interest. There is no need to simplify the system of ODEs to accommodate SP, and decreasing the sizes of the intermediate time steps increases the precision of the solution (to a lower bound limited by numerical precision). Thus, SP is capable of obtaining the greatest accuracy of the three classes. The cost is that decreasing the time step increases the number of required evaluations of the system of ODEs, a significant burden because of the time-consuming calculations required by high-fidelity dynamics models.

On the other hand, a general perturbation (GP) method does not "propagate" the SO state by stepping sequentially in the independent variable t from t_i to t_{i+1} to $t_{i+2}\ldots$ until reaching some desired t_f. Instead, the state at any t is calculated as an explicit function of the initial state. As a result, a GP method can generate a long-term state prediction much more rapidly than an SP method. The downside, of course, is that any analytical solution is necessarily a more coarse approximation of the true dynamics than a high-fidelity SP model.

Semianalytical methods seek to provide greater accuracy than fully analytical GP methods without the high computational cost of SP methods. Unlike in a GP method, the ODEs of a semianalytical

description of the dynamics are not solvable analytically; however, the system is formulated such that the states vary slowly enough that the step sizes used by a numerical propagator may be much larger than those of an SP method for comparable truncation error [2].

SP, GP, and semianalytical methods are all applicable to SO translation (the three-degree-of-freedom or 3DOF problem), rotation, or coupled translational/rotational motion (the 6DOF problem). The last of these dynamical regimes is the subject of the present work. Accordingly, the approach is deemed a *hybrid* SP/GP technique for 6DOF SO propagation. Specifically, SO attitude is calculated using a GP method, and this approximation is used to inform an SP propagation of the 3DOF state. The development of this approach is motivated chiefly by two factors:

1) 6DOF SP propagation is notoriously slow due to factors such as 1) the increased size of the state vector, 2) the use of potentially complicated SO shape models for the calculation of body forces and torques, and 3) differences between the characteristic time scales of the translational and rotational dynamics [3]. Using GP to approximate SO attitude allows for the removal of the rotational state from the numerically propagated state vector. This change significantly increases the efficiency of the overall state prediction because the numerical propagator is less influenced by the fast time scales of the rotational dynamics. The hybrid method may thus also be considered a semianalytical technique [4].

2) In many cases, greater accuracy is desired in the prediction of the 3DOF state than in the rotational state (e.g., catalog maintenance, conjunction analysis). However, body forces like those caused by aerodynamic drag and solar radiation pressure (SRP) depend on SO attitude. Thus, even though the GP attitude prediction is not high fidelity, the 3DOF state prediction may be improved by using a better approximation of the attitude than would be available from the common "cannonball" assumption. Approximate knowledge of SO attitude can be valuable for applications such as active debris removal [5–7]. The hybrid method therefore serves as a middle ground between 3DOF and 6DOF SP methods.

The overall hybrid method is independent of the closed-form attitude solution, which allows a practitioner to select from available solutions a method that meets their needs. In the current work, a specific solution is implemented to numerically demonstrate the capabilities of the hybrid method [8,9]. The solution is derived using the Lie-Deprit Hamiltonian perturbation theory [10] and assumes a fast-rotating, triaxial SO in an elliptical orbit subject to gravity-gradient torque. Algorithmic elements unique to this attitude solution are discussed. The hybrid method is compared against SP 3DOF-only and fully coupled 6DOF propagations for 1) a tumbling rocket body in low Earth orbit (LEO) and 2) a high-area-to-mass-ratio (HAMR) SO in a geostationary transfer orbit (GTO). These two scenarios are chosen because of their practical importance, sensitivity to attitude variations, and the assumptions of the specific closed-form attitude solution. First, the prevalence and large size of disposed rocket bodies in Earth orbit make them primary targets for active debris removal. Any generic active debris removal strategy would benefit from the approximate knowledge of a target SO's attitude that the hybrid propagation method provides [5–7]. Second, HAMR objects are significantly disturbed by body forces and torques. If the SO surface area changes over time, the invalidity of the cannonball assumption of a 3DOF propagation is therefore more detrimental to the accuracy of state prediction for a HAMR SO than for other types of SOs [3].

In the context of the simulation results for these two example scenarios, practical aspects of using the hybrid method are discussed, including the identification of regions in the accuracy versus compute-time space in which the hybrid method is most attractive. This concept is particularly important because such identification is necessary to achieve strong performance with the hybrid method, and the region of interest is not necessarily the same for all scenarios.

Before a more detailed discussion of the hybrid method, the concept of semianalytical methods for translational motion is introduced. Additionally, as the hybrid method requires a closed-form solution for the rotational motion of an SO, a brief review of selected theories is presented. Several previous efforts to improve the efficiency of 6DOF propagation by partially decoupling the translational and rotational dynamics are also discussed.

A. Semianalytical Methods for Space Object Translational Dynamics

As previously mentioned, semianalytical techniques provide greater accuracy than fully analytical GP methods without the high computational cost of SP methods. This property is realized by simplifying the high-fidelity system of ODEs used by SP without requiring that the new system have an analytical solution—thereby admitting more complicated dynamics models than GP methods. For instance, Draper Semianalytic Satellite Theory (DSST) uses both analytical and numerical averaging procedures to derive a system of ODEs for a set of mean orbital elements [4]. The method of multiple scales [11] has also been used to produce semianalytical models [12]. While the ODEs are not solvable analytically, the states vary slowly enough that the step sizes used by a numerical propagator may be much larger than those of an SP method for comparable truncation errors [2].

B. Analytical Methods for Space Object Rotational Dynamics

Despite the ever-increasing capabilities of computers, GP methods for both translational and rotational state prediction remain valuable for several reasons. First, the speed of GP methods is still unmatched by their SP counterparts. Thus, for applications in which many predictions are required—and extreme accuracy is not—GP is strongly preferable to SP. For the same reason, GP methods are indispensable for very long-timespan state predictions. Additionally, the analytical expressions produced by GP can often provide more insight into the general behavior of a class of SO than the coupled ODEs used by SP methods.

A frequently studied scenario is the rotation of an SO subject to gravity-gradient torque due to the importance of this disturbance in LEO [13]. Holland and Sperling [14] directly average Euler's equation for the time derivative of the rotational angular momentum of a rigid body [15] to obtain a first-order solution for the evolution of the angular momentum vector of an SO subject to gravity-gradient and geomagnetic torques (under certain assumptions). Unfortunately, the theory does not predict the actual orientation of the SO. Crenshaw and Fitzpatrick [16] use the Hamilton-Jacobi equation to obtain a transformation from Euler angles and momenta to a set of variables that are constant for a symmetric rigid body in torque-free rotation. In these variables, the authors use the method of successive approximations to obtain the same first-order solution for an SO subject to gravity-gradient torque as Holland and Sperling [14], but add expressions for the SO orientation. Hitzl and Breakwell [17] use a canonical transformation to write the Hamiltonian for a torque-free, triaxial rigid body independent of coordinates. The gravity-gradient perturbation (assuming an elliptical orbit) is added to the Hamiltonian, and short-period terms are removed through direct averaging, which allows for the determination of the secular rates of the transformed variables. Cochran [18] extends the work of Hitzl and Breakwell [17] to the case of a secularly precessing elliptical orbit. Each of the preceding theories assumes that the rotation rate of the SO is large compared with the orbital rate, and a value related to the ratio of the mean motion to the rotational speed of the SO is used as the small parameter of the perturbation theories.

More recently, Lara and Ferrer [8], explicitly referring to this problem as that of a fast-rotating satellite, derived a form of the coordinate-free Hamiltonian in terms of action-angle variables, under the assumption of a triaxial SO in a circular orbit. The Lie-Deprit transformation procedure [10] is then used to compute a first-order solution that, unlike the previous works, retains the short-period terms. Additionally, the use of action-angle variables eliminates the appearance of mixed secular-periodic terms in the transformation equations. Lara, Ferrer, and coauthors have also applied perturbation theory to other, similar cases, including the rotation of a symmetric SO in a circular orbit subject to gravity-gradient torque [19]. A first-order solution is derived equivalently using both the method of successive approximations and the Lie-Deprit method. Additionally, Lara et al. [20] investigate the rotation of the dwarf planet Ceres due

to the gravity-gradient torque of the Sun. The Lie-Deprit method is used to derive an analytical solution in which the nonsphericity of Ceres is treated as a perturbation and the eccentricity of Ceres's orbit is taken into account.

Meanwhile, San-Juan et al. [21] use the Lie-Deprit method to obtain a higher-order solution for a symmetric SO in a circular orbit. Despite the fact that two is the maximum order present in the original perturbed Hamiltonian, improved accuracy in the perturbation solution is achieved by retaining terms up to fourth-order in the transformed Hamiltonian.

GP solutions for other scenarios have also been put forth. For example, Van der Ha [22] uses the method of successive approximations to derive a second-order solution for an SO subject to a torque that is constant in the body-fixed reference frame. Zanardi and coauthors have presented several analytical theories, including a first-order solution assuming gravity-gradient and SRP torques (with no Earth shadow) [23]; an orbit-averaged solution for a spin-stabilized SO subject to magnetic residual torque [24]; and a first-order solution for a gravity-gradient-perturbed SO in nonsingular variables [25]. In each case, the perturbation solution is obtained using variation of parameters and the method of successive approximations. Bois and Kovalevsky [26] also use the method of successive approximations, producing first-order [27] and second-order [28] solutions for the rotation of a triaxial satellite subject to arbitrary torques. The solution represents the torques as Fourier series in the Euler angles describing the orientation of the body and additional angles (such as the SO-Sun angle) that are assumed to vary linearly in time; the coefficients of the series must be determined by the practitioner for each application. Though the theory does not assume fast rotation, deviations from rotation about a single spin axis are assumed to remain small.

In addition to the work previously described for predicting translational and rotational motion individually, the perturbation framework has been applied to the roto-translational problem to obtain a GP solution for full 6DOF motion. These theories are not specifically the subject of this paper due to a desire for higher-fidelity prediction of translational motion. However, as with the translation-only GP methods, it is appropriate to mention several examples because of similarities between the 6DOF theories and the perturbation theories developed in this paper.

Ferrandiz and Sansaturio [29] use the Lie-Deprit method to obtain a first-order, average 6DOF solution for a quasi-spherical SO in a Keplerian orbit. This solution is subsequently extended to the case of an oblate central body [30]. Ferrer and Lara [31] use both the Lie-Deprit method and transformations based on the Hamilton-Jacobi equation to address the case of an axisymmetric SO in a Keplerian orbit. Finally, the Lie-Deprit method is also used by Mohmmed et al. [32] to develop a theory for a cylindrical SO that takes into account central-body oblateness and geomagnetic torque. The nonconservative geomagnetic torque is introduced to the Hamiltonian through a "potential-like" function.

As may be expected, the increased dimensionality of the 6DOF problem compared with the independent translational or rotational problems generally leads to the appearance of significantly more terms in the perturbation solutions.

C. Partial Decoupling of 6DOF Dynamics

The hybrid method seeks to reduce the dependency of the step size of the state prediction ODE solver on the rotational dynamics by analytically predicting the rotational state. Several previous methods have attempted to do likewise by partially decoupling the translational and rotational dynamics. For example, multiple variations of an Encke-type algorithm have been proposed.[‡] In one such approach, forces independent and dependent on SO attitude are separated from one another in the translational equations of motion [34,35]. The Encke reference trajectory is taken to be the numerically propagated solution obtained using only attitude-independent forces, which is assumed to take larger step sizes than a coupled orbit/attitude state due to the assumed high frequencies of the rotational motion. Once a step is taken in the reference propagation, the rotational state and corrections to the translational state are propagated using the necessary smaller step sizes, with the reference translational state obtained as needed via interpolation. In this way, unnecessary evaluations of attitude-independent forces are avoided. Naturally, efficiency improvements depend heavily on the relative expenses of the attitude-dependent and attitude-independent dynamics. For example, the combination of a high-degree/order geopotential and a simple SO physical model is likely to lead to strong efficiency gains, while the opposite situation may result in minimal speed increases. In one test simulation in which dynamics evaluation times were dominated by a spherical harmonics geopotential calculation, efficiency gains of approximately 3× and 4× over a fully coupled propagation were reported for 36×36 and 50×50 fields, respectively [34].

A related method performs the "long-step" propagation using an assumption of constant angular velocity, while the attitude propagation is performed assuming a Keplerian orbit [3]. The two systems are recoupled each time a threshold value of a measure of separation between the two propagations is exceeded, and the split propagations are begun anew. Simulations of a slowly rotating, HAMR SO in a near-geosynchronous orbit have demonstrated CPU time savings of approximately 10% relative to a fully coupled propagation.

II. Hybrid SP/GP Method for 6DOF SO State Prediction

A step-by-step description of the hybrid algorithm is given below; the process is summarized in Fig. 1.

1) Given an initial time, 6DOF state, and constants (e.g., SO inertia tensor), values are calculated for the expressions needed by the closed-form rotational state prediction procedure.

2) A numerical ODE solution routine is initialized. The state vector of propagation contains only the 3DOF SO state.

3) Criteria (if any) for reinitializing the closed-form rotational state prediction are defined. Reinitialization of the closed-form attitude solution algorithm may be desirable if the SO state evolves such that the values calculated in the most recent execution of step 1 no longer adequately represent the scenario.

4) At each propagation step, the ODE solver calls a routine to evaluate the translational state equations $\boldsymbol{f}_{\text{tr}}$ one or more times. Each evaluation requires the calculation of the external forces acting on the SO at the current time and state. While the 3DOF state is obtained from the propagation of the solution of the system of ODEs, the rotational state is obtained by evaluating the analytical attitude solution at the given time. This strategy requires that the values calculated in step 1 be available to the $\boldsymbol{f}_{\text{tr}}$ evaluation routine in some form.

5) If necessary, step 1 is repeated (see step 3).

6) If desired, the values of the rotational state at each propagation step may be output and saved.

The specific method used to predict the rotational state is irrelevant to the algorithm, as long as the prediction is a closed-form function of time and initial conditions only. The method may therefore be selected by the practitioner based on considerations such as 1) applicability to physical/dynamical conditions, 2) ease of implementation, and 3) computational efficiency. As an illustration of the hybrid method, SO attitude is calculated in this work using the solution of Lara and Ferrer [8] for a fast-rotating, triaxial rigid body subject to gravity-gradient torque. The solution, originally applicable to circular orbits only, has been extended by the present authors to apply to elliptical orbits [9].

Once a rotational GP solution is selected, any points specific to that theory must be addressed. For the fast-rotating, gravity-gradient solution, such considerations include the following:

1) The Hamiltonian is initially formulated using Andoyer variables [15,36], and so transformations between the Andoyer set and any

[‡]In the traditional Encke method for 3DOF propagation, a known reference solution is calculated analytically, and a numerical ODE solver is applied only to deviations from the reference trajectory [33].

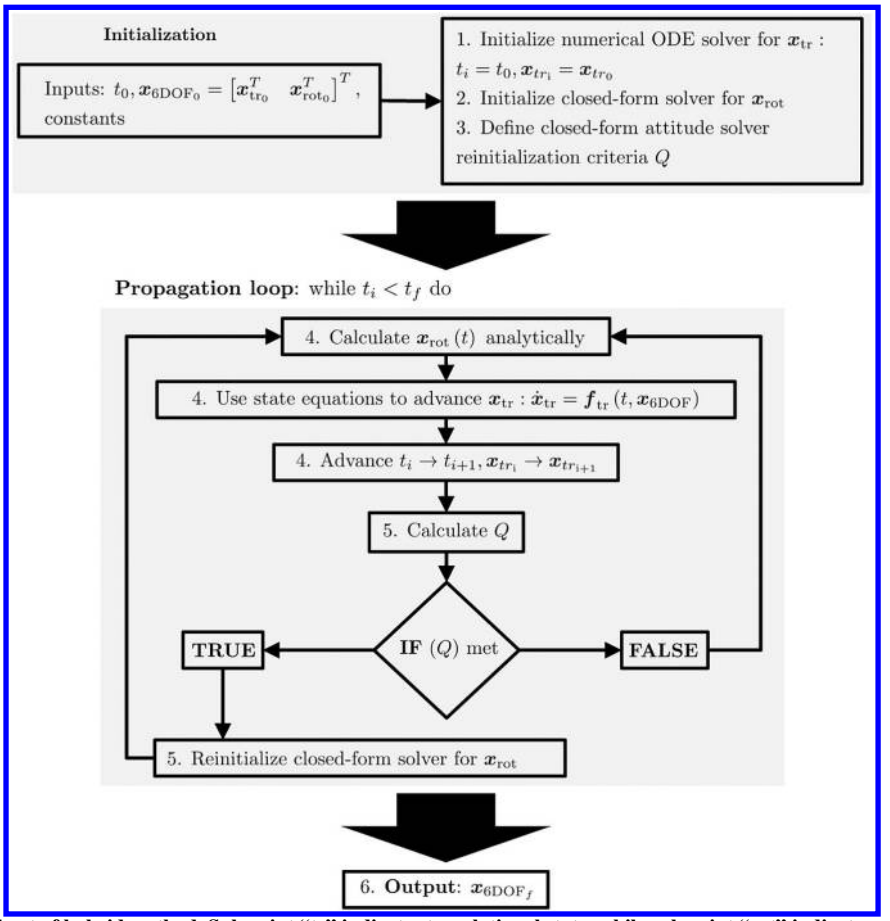

Fig. 1 Flow chart of hybrid method. Subscript "tr" indicates translational state, while subscript "rot" indicates rotational state.

other desired attitude representations (e.g., a transformation matrix) must be implemented. Additionally, the Andoyer variables are singular for certain SO configurations, and so a transformation to an alternative set of variables must be performed if it is expected that a singularity condition may be encountered [37].

2) Averaging over an angle implicitly assumes that the angle circulates; this criterion must be met by all angles over which averaging is performed.

3) The perturbation solution is found by performing the Lie-Deprit transformation procedure twice in succession, each time to eliminate the terms in the Hamiltonian that are periodic in a different variable. As a result, there are actually three possibilities for calculating a solution in the untransformed variables once the solution is obtained in the transformed, "doubly averaged" variables:

a) transform directly from the doubly averaged variables to Andoyer variables;

b) transform from doubly averaged to singly averaged variables before transforming to Andoyer variables;

c) transform from doubly averaged to singly averaged variables, and from singly averaged to unaveraged variables before transforming to Andoyer variables.

As the number of transformations increases, the amount of periodicity recovered in the solution increases as well. However, computational effort also increases. The impact of which transformation strategy is chosen is investigated in the numerical examples in the Results section.

4) The transformation equations of the perturbation theory rely on elliptic integrals and Jacobi elliptic functions; a satisfactory implementation of these functions is therefore required [38–42].

Regardless of which GP method is selected, the accuracy of the hybrid method is strongly dependent on how well the assumptions of the analytical attitude solution are met. In the present case, the most important assumptions are:

1) The SO is rotating quickly, in the sense that the assumptions of the averaging procedure are valid [8].

2) The parameter of the perturbation procedure, ϵ, is small.[§]

3) Gravity-gradient torque is the only torque acting on the SO.

4) The SO is in a Keplerian, elliptical orbit.

Assumptions (1), (2), and (4) are functions of the initial conditions and mass properties of the SO. For an Earth-orbiting SO, assumption (3) is never completely valid due to the presence of torques caused by aerodynamic drag, SRP, the Earth's magnetic field, and so on. Thus, the validity of the assumption must be assessed on a case-by-case basis, taking into account such factors as SO mass properties, reflectance properties, and electromagnetic properties, as well as the orbit regime.

Assumption (4) is not strictly valid for any force model other than a simple two-body model. However, this issue may be circumvented to some extent because orbital perturbations generally cause slow changes to an initial osculating Keplerian orbit. Closed-form solution values calculated using an initial reference orbit may therefore be used to predict rotational states without significantly compromising accuracy as long as the osculating orbit at the time of prediction does not deviate substantially from the reference orbit. If the deviation becomes too large, the reference orbit may be reselected based on the current state, and the expressions used to calculate the rotational state as a function of time may be reinitialized. (The initial time used by the closed-form solution must be updated as well.)

While it is feasible to reinitialize the reference orbit at *every* time step, frequent updates can lead to undesirable side effects. First, the efficiency of the overall propagation is worsened due to the increased number of computations. Second, if a new reference orbit is selected too frequently, the quality of the attitude solution actually degrades, even though the validity of assumption (4) improves. The reason is that the Lie-Deprit transformation procedure used to obtain the perturbation solution is truncated at first order. Therefore, when the transformed variables generated by the solution procedure (the $\boldsymbol{\xi}''$)

[§]Assumptions (1) and (2) are related, but not identical.

are converted back to untransformed variables (the $\boldsymbol{\xi}$), some information is lost. The problem is exacerbated if these new untransformed variables are then, in turn, used to perform step 1 of the hybrid algorithm. It is thus advisable to change the reference orbit prudently.

In the examples presented in the current work, the decision to reinitialize the reference orbit is based on the duration since the most recent initialization, measured in units of the orbital period. The time between reinitializations is set before propagation and held constant. More sophisticated criteria are possible, such as a metric that measures a "distance" between the current osculating orbit and the most recent reference orbit. It is important that the selected criterion may be computed quickly to preserve the efficiency of the hybrid method.

III. Results

Numerical results are presented to demonstrate the utility of the hybrid method. First, the GP solution for rotation is isolated to assess its computational cost. Then, two case studies are presented to show that 1) the assumptions of this hybrid method implementation are met for realistic and important scenarios and 2) the hybrid method provides a meaningful bridge between 3DOF and 6DOF SP methods for these scenarios.

SP-based attitude propagation is performed by modeling an SO as a collection of one or more rigid, flat plates. The numerical solution of systems of ODEs is calculated using the LSODE package, which provides an open-source, variable-step-size, variable-order, linear-multistep (Adams method) ODE solver [43]. A reference "truth" solution is generated using a quadruple-precision implementation of the full 6DOF system. For the hybrid method, a new reference orbit is generated once per orbit period; in testing for both case studies, this frequency was found to be a reasonable implementation that balances the accuracy of the assumptions of the closed-form solution and computational effort and inaccuracies caused by overly frequent coordinate transformations.

All code is written in Fortran and compiled using the Intel Visual Fortran Compiler XE 14.0.0.103 (64-bit) using the $-O_2$ optimization flag. All computations are performed on a 64-bit Windows 7 Enterprise workstation with two 12-core Intel Xeon E5-2680 v3 processors (clock speed 2.50 GHz) and 64 GB of RAM. Hyperthreading is disabled.

A. Computational Speed of Closed-Form Attitude Solution

The computational times required to perform the various transformations of the closed-form attitude theory are depicted in Fig. 2 to help practitioners calibrate the CPU effort.[¶] Times are normalized by the compute time of the 8×8 gravitational acceleration (spherical harmonics implementation), and the meanings of the abbreviations used in the legend of Fig. 2 are given in Table 1. Note that $\bar{\boldsymbol{q}}$ and $\boldsymbol{\omega}$ are the quaternion and angular velocity vector representations of the attitude and attitude rates, respectively, needed for evaluation of attitude-dependent 3DOF acceleration terms. Additionally, $\boldsymbol{\xi}, \boldsymbol{\xi}'$, and $\boldsymbol{\xi}''$ are the solution variables, the singly transformed variables, and the doubly transformed variables of the closed-form theory, respectively; a dot represents a time derivative. The data points shown in Fig. 2 represent the various transformation levels of the closed-form theory described in the previous section.

Predictably, as the number of transformations increases, so does the compute time: The three transformation levels (0, 1, and 2) are approximately equivalent to spherical harmonics acceleration calculations of degree and order 11, 13, and 16, respectively, while the initialization procedure is roughly equivalent to a degree and order 14 calculation. It is therefore important to perform only those transformations that result in significant improvements in solution accuracy. Additionally, the overall computational cost of the dynamics model must be taken into account when deciding whether or not to use the hybrid method. A very inexpensive dynamics model may see little or no speed increase from the hybrid method compared with a full 6DOF propagation.

[¶]All CPU times are averaged over a number of trials such that the total compute time for each case is greater than 1 s.

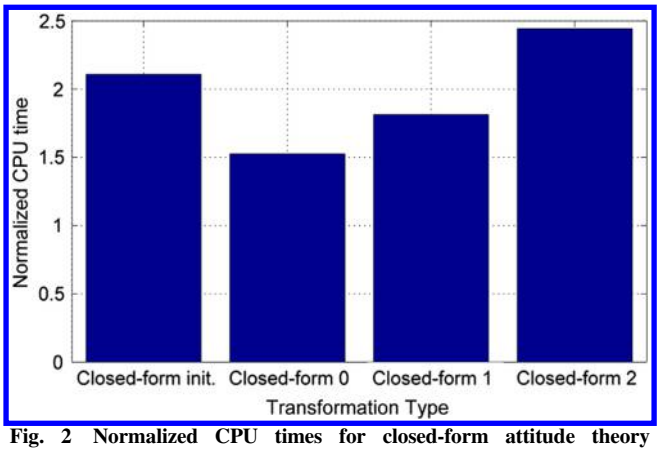

Fig. 2 Normalized CPU times for closed-form attitude theory operations. (One time unit $= 1.29\ \mu$s.)

Faster analytical solutions may be feasible depending on the specific scenario. For the current closed-form theory, a significant driver of compute time is the calculation of elliptic functions and integrals, which appear due to the triaxiality of the body. If the body is axisymmetric, alternative theories that rely only on trigonometric functions are available [19]. For a nearly axisymmetric body, a small triaxiality may be treated as a perturbation, and again a closed-form theory in terms of trigonometric functions may be derived [20]. Alternatively, a closed-form theory based on perturbation methods is available for an arbitrarily triaxial body provided that the body is experiencing short-axis-mode rotation (i.e., rotation nearly entirely about the body's axis of maximum inertia [44]) [45,46]. As in the other simplified cases discussed here, the relevant equations are based on trigonometric functions. Such simplifications, when applicable, improve the efficiency of the closed-form solution [41].

B. Tumbling Rocket Body in LEO

The first example application simulates 15 orbits of a rocket body SO in LEO. The physical properties of the SO are based on a Centaur upper stage, approximately modeled as a cylinder with length 12.68 m, diameter 3.05 m, and inert mass 2243 kg [47]. To induce a larger aerodynamic drag torque than would otherwise be generated, the center of mass of the SO is moved away from the geometrical center by 0.634 m along the long axis. This modification is made so that the simulation yields a more conservative demonstration of the hybrid method's capabilities: The closed-form attitude solution takes into account only gravity-gradient torque, and so aerodynamic torque creates attitude modeling inaccuracies for the hybrid method. It is also noted that, for a derelict rocket body, the center of mass is very likely to be offset from the geometric center because, while a significant amount of fuel has been expended, the motor itself (which is not centered within the body) remains. A small asymmetry in the radial plane of the SO is introduced, as shown in Table 2a, in order to conform to the triaxiality assumption of the closed-form attitude theory.

The SO orbit is based on that of a Centaur SO launched in 1972 and still in LEO today (NORAD ID 6155); Table 2b gives the initial orbital state used in this example [48]. The initial rotational state assumes a primary tumbling motion about the axis of greatest inertia, with a rotational period of approximately 32 s. This rotation rate is not necessarily the realistic value, but rotation rates of similar magnitudes have been estimated for disposed rocket bodies using light curves [5,49,50]. The initial rotational state of the body-fixed frame with respect to the Earth-centered inertial (ECI) frame (equatorial J2000) is given in Table 2c.

The 3DOF force model consists of a 70×70 spherical harmonics implementation of the geopotential, aerodynamic drag, and point-mass lunisolar gravitational forces. Atmospheric density is calculated using an upgraded version of the modified Harris-Priester method [51,52]. For fully numerical 6DOF propagations, torques caused by

Table 1 Summary of coordinate transformations

Fig. 2 label	Transformation	Description
Closed-form init.	$\bar{\boldsymbol{q}}, \boldsymbol{\omega} \rightarrow \dot{\boldsymbol{\xi}}''$	Initialization transformation: 3DOF attitude acceleration variables → closed-form attitude solution variables
Closed-form 0	$\dot{\boldsymbol{\xi}}'' \rightarrow \boldsymbol{\xi}'' \rightarrow \bar{\boldsymbol{q}}, \boldsymbol{\omega}$	Solution variables → 3DOF acceleration variables (direct)
Closed-form 1	$\dot{\boldsymbol{\xi}}'' \rightarrow \boldsymbol{\xi}'' \rightarrow \boldsymbol{\xi}' \rightarrow \bar{\boldsymbol{q}}, \boldsymbol{\omega}$	Solution variables → 3DOF acceleration variables (one intermediate transformation)
Closed-form 2	$\dot{\boldsymbol{\xi}}'' \rightarrow \boldsymbol{\xi}'' \rightarrow \boldsymbol{\xi}' \rightarrow \boldsymbol{\xi} \rightarrow \bar{\boldsymbol{q}}, \boldsymbol{\omega}$	Solution variables → 3DOF acceleration variables (two intermediate transformations)

Table 2 Parameters defining rocket body SO example simulation

a) Inertia tensor elements along principal axes in body-fixed frame	
A	6593.76 kg · m^2
B	40492.81 kg · m^2
C	40658.00 kg · m^2
b) Initial orbital state	
a	7042.35 km
e	0.00374
i	35.0 deg
Ω	122.0 deg
ω	237.0 deg
ν	0.0 deg
c) Initial rotational state	
q_1	0.0596
q_2	0.0132
q_3	0.2667
q_4	0.9618
ϕ	28 deg
θ	7 deg
ψ	3 deg
$\boldsymbol{\omega}_x$	0.1146 deg/s
$\boldsymbol{\omega}_y$	1.1459 deg/s
$\boldsymbol{\omega}_z$	11.2511 deg/s

the gravity gradient and aerodynamic drag are considered; the hybrid method takes into account only the averaged gravity-gradient torque. For the purposes of calculating body forces (for the fully numerical 6DOF and hybrid methods) and torques (for the fully numerical 6DOF method only), the SO is modeled using six flat, rigid panels arranged as a rectangular prism, with side lengths 12.68 m, 3.0 m, and 3.1 m. For 6DOF and hybrid propagations, the algorithm of Doornbos is used to calculate individual lift and drag coefficients for each panel; for 3DOF propagations, the Doornbos method is integrated in closed form assuming a uniform, spherical SO to obtain a single drag coefficient [53] (i.e., cannonball-based drag). This method produces a calculated drag coefficient rather than relying on a user-specified value. While the use of more panels could better approximate a cylinder (or a shape closer to a true rocket body, including nozzles, etc.), this simple model is sufficient for a demonstration of the hybrid methodology. This physical model is also representative of the level of modeling that might be used if limited SO body information is known.

If a significantly higher-fidelity physical model (i.e., one made up of many more individual panels) is available, the practitioner has multiple options when using the hybrid method. First, the hybrid may employ the high-fidelity shape model. In this case, while the efficiency advantage of the hybrid method over fully numerical 6DOF propagation remains, the computational expense of *either* relative to 3DOF propagation increases due to the calculation of body forces on a large number of surfaces. An alternative is to use a lower-fidelity, approximate shape model with the hybrid method. This strategy is also an option for obtaining faster, less-accurate state predictions using full 6DOF propagation, but is particularly synergistic with the hybrid method because the latter is based on efficiency-improving approximations.

A key consideration in comparing a 3DOF propagation of the system to either a 6DOF or hybrid propagation is the surface area value used to calculate aerodynamic drag. For the 6DOF or hybrid model, the area of each panel exposed to the atmosphere is calculated dynamically as a function of the attitude, but the 3DOF model has no such information. Therefore, a constant area is assumed. In the results presented in this study, two constant area values are used. First, a quick, rough value is obtained by averaging the areas of the sides of the rectangular prism model (28.88 m^2). Second, the area value that produces the smallest root-mean-square (RMS) error relative to the 6DOF reference solution over the course of the propagation is determined numerically using a grid search; this value is found to be 41.85 m^2. This second method is not feasible in a practical scenario, but is included to provide a best-case scenario for the accuracy achievable by the cannonball model.

Simulation results for the 15-orbit propagation are summarized in Figs. 3 and 4, which show RMS position state errors over the propagation period relative to the 6DOF "truth" reference propagation as a function of CPU time for a range of relative tolerances for the ODE solver.** (Values for the 3DOF solvers are shown alongside the 6DOF and hybrid solvers because only the position state is considered in this plot.) The 0, 1, and 2 subscripts of "Hybrid" in the legend have the same meanings as the 0, 1, and 2 labels for "Closed-form" given in Table 1 for the closed-form attitude solution. The 3DOF legend entry with no subscript indicates that the averaged area is used, whereas the "Best A" subscript indicates that the numerically determined lowest-error area is used. Finally, results for two full 6DOF propagations are presented. The subscript "All" indicates that the same relative tolerance is used for all states in the ODE solver. Meanwhile, the subscript "Low" means that the relative tolerance on the rotational states is held fixed at 10^{-3} while the tolerance on the translational states is varied. The latter option is included for comparison because it mimics the ideology of the hybrid method by producing a lower-fidelity attitude solution alongside a more precise translational solution.

In the present work, the primary point under investigation is the capability of the hybrid method to improve translational state prediction by using approximated attitude states to calculate body forces. Thus, discussion of the accuracy of the full 6DOF state prediction is limited. However, more detailed information on the performance of the particular closed-form attitude solution used here may be found in Refs. [8,9,54].

The two styles of 3DOF propagation behave similarly except for an improvement in accuracy when the optimized drag area is used. Each is inexpensive relative to the 6DOF and, to a lesser extent, hybrid propagations. However, the 3DOF solutions reach a relatively high "accuracy floor," at which point reducing the tolerance of the ODE solver no longer produces a more accurate solution. For the averaged-area propagation, the minimum RMS error is approximately 66 m, whereas, for the best-area propagation, the minimum RMS error is approximately 20 m.

For the fully numerical 6DOF propagation, the accuracy of the "Low" version increases without a corresponding increase in CPU time over the majority of the translational state integration tolerance range. The reason is that the tolerance on the rotational state, though held at a loose value, nevertheless drives the step size of the propagation until the translational relative tolerance is less than or equal to 10^{-13}. Alternatively, the CPU time for the "All" version

**That is, each solution method is executed multiple times with each run using a different relative tolerance value for the ODE solver. Changing the relative tolerance changes the number of steps taken by the ODE solver and thus the CPU time required, resulting in multiple data points for each solution method.

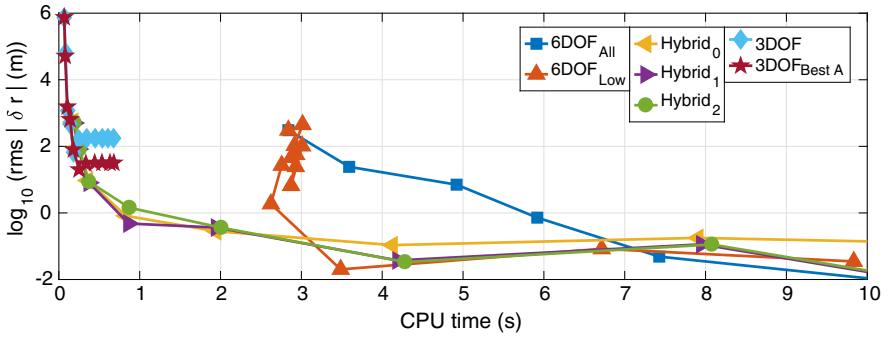

Fig. 3 RMS position error as a function of CPU time for 15-orbit propagation of a rocket body in LEO.

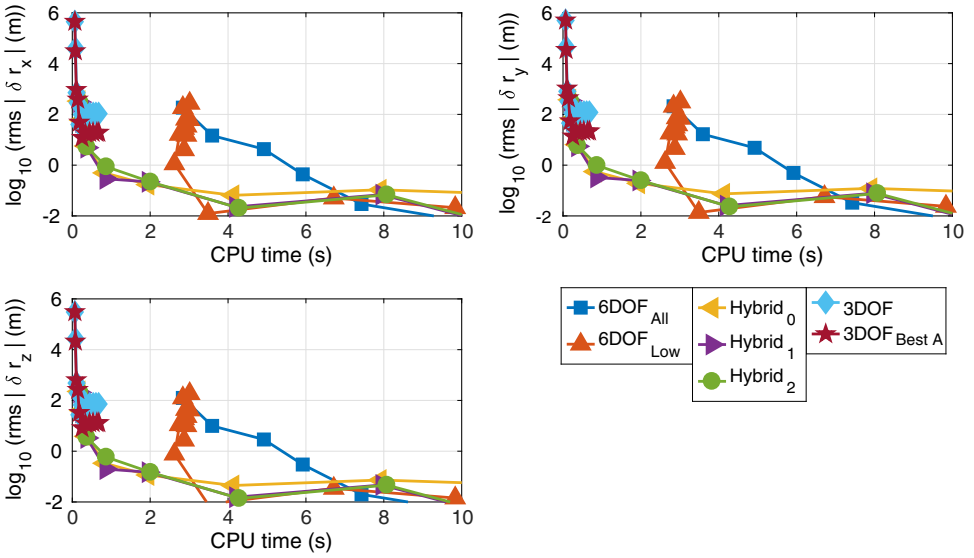

Fig. 4 ECI componentwise RMS position error as a function of CPU time for 15-orbit propagation of a rocket body in LEO.

increases with each decrease in tolerance. As a result, the accuracy floor of the "All" propagation is more than two orders of magnitude smaller than that of the "Low" propagation, but a CPU time of about 14 s is required to reach the smaller floor.[††]

The utility of the hybrid method is visible in the lower left portion of Fig. 3, in which the hybrid method offers a solution that is more accurate than the best-area 3DOF propagation and faster than the "Low" 6DOF propagation. The hybrid method (regardless of transformation level) achieves approximately meter-level accuracy—more than an order of magnitude below the accuracy floor of the best-area 3DOF solution—using about three and six times less CPU time than the "Low" and "All" 6DOF methods, respectively.

At the same time, notes of caution regarding use of the hybrid method must be mentioned. First, appropriate integration tolerance (or step size) selection for the ODE solver used to propagate the translational equations of motion is important. Excessively loose tolerances (or large step sizes) produce results no more accurate than a 3DOF propagation, while excessively tight tolerances (or small step sizes) result in less accuracy for a given CPU time than a full 6DOF propagation. For this example, the relative tolerance "sweet spot" is approximately 10^{-10} to 10^{-12}.

Second, the choice of transformation type used by the attitude solution (0, 1, or 2) impacts the accuracy and efficiency of the propagation, though the speed variation is not large for the current example due to the expense of the translational dynamics model. Over the range of tolerances in which the hybrid method is beneficial for this example, there is little difference in accuracy between the transformation types, as well. However, as shown in Fig. 5, differences do exist: Primarily, transformation types 1 and 2 tend to provide similar accuracies, while less accuracy is obtained from transformation type 0. This result is examined in further detail in the commentary of the second example application.

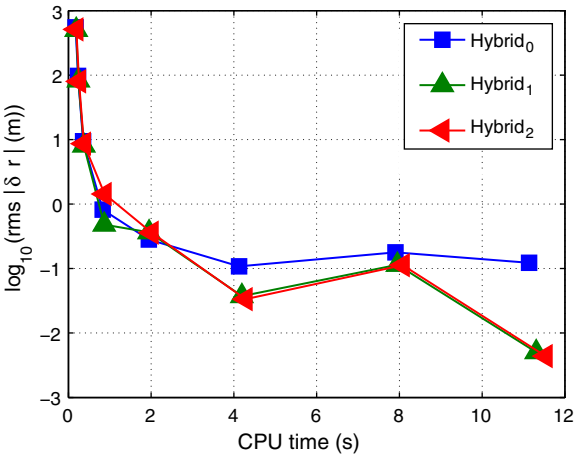

Fig. 5 Simplification of Fig. 3, featuring only the hybrid solutions and extending the CPU time axis to show all data points.

[††]Note that the CPU time axes in Figs. 3 and 4 are truncated to improve readability in the regions of greatest interest, and the accuracy floor of the "All" propagation is not visible in the plots.

Table 3 Common logarithm (i.e., $\log_{10}$) of ODE solver relative tolerances corresponding to data points in Fig. 6

	ODE solver tolerance				
Initial ω_z, deg/s	Hybrid_0	Hybrid_1	Hybrid_2	6DOF_{All}	6DOF_{Low}
11.2511	−10.2	−10.2	−10.2	−4.8	−11.6
22.5021	−10	−10	−10	−5	−12.6
33.7532	−10	−10.2	−10	−4.2	−10
45.0042	−10.2	−10	−10.2	−4.2	−10.2
56.2553	−10	−10.2	−10	−4.2	−9.2
67.5063	−10	−10.2	−10	−4.2	−8.8
78.7574	−10.2	−10.4	−10	−4.2	−9
90.0084	−10	−10.4	−10	−4	−9
101.2595	−10	−10	−10	−4	−9
112.5105	−10.2	−10	−10.2	−4	−9.2

1. *Impact of SO Rotation Rate*

The rocket body scenario is re-simulated for integer multiples of the initial primary spin rate ($\boldsymbol{\omega}_z$) ranging from 1 to 10 (see the leftmost column of Table 3). Each propagation scheme is run for a range of ODE solver relative tolerance values: $\text{tol} = 10^x$, with x varied in increments of 0.2 (i.e., $\ldots, 10^{-9}, 10^{-9.2}, 10^{-9.4}, \ldots$). For the hybrid and 6DOF variations, the loosest ODE solver tolerance that results in an RMS position error smaller than 7 m is identified. This cutoff value is chosen because it corresponds to an improvement of approximately one order of magnitude over the best-case accuracy obtained by the 3DOF propagation using an average area value (see Fig. 3). The selected tolerances for each case are given in Table 3. For these specific runs, the speedups of the 6DOF "Low," Hybrid_0, Hybrid_1, and Hybrid_2 propagations relative to the 6DOF "All" propagation are shown in Fig. 6.

This parameter sweep demonstrates how the hybrid method becomes more effective as the rotation rate of the SO increases: The relative speedups of the hybrid method increase from approximately 10× to greater than 80× over the range of initial spin rates plotted in Fig. 6. Meanwhile, the relative speedups achieved by the "Low" 6DOF option remain relatively constant between 1.5× and 1.8× as the initial spin rate increases.

A faster rotation rate means that a fully numerical 6DOF propagation must take smaller time steps to capture the high-frequency changes in the rotational state. The hybrid method is less affected by such changes because the rotational state is calculated analytically. The increased spin rate is therefore only important to the step sizes taken by the hybrid method inasmuch as the time evolution of body forces acting on the SO changes.

The accuracy of the rotational state predictions of the hybrid method improves as the spin rate increases because the closed-form attitude solution assumes fast rotation. However, even the slowest spin rate considered in this case study is fast enough that the effect on the overall accuracy of the predicted position state is minimal over the 15-orbit prediction time span.

Table 4 Parameters defining HAMR SO example simulation

a) Inertia tensor elements along principal axes in body-fixed frame	
A	2.47×10^{-5} kg · m^2
B	9.90×10^{-5} kg · m^2
C	1.23×10^{-4} kg · m^2
b) Initial orbital state	
a	24009.05 km
e	0.713
i	20.6 deg
Ω	198.0 deg
ω	109.0 deg
ν	0.0 deg
c) Initial rotational state	
q_1	0.0727
q_2	0.0481
q_3	0.5926
q_4	0.8008
ϕ	70 deg
θ	10 deg
ψ	3 deg
$\boldsymbol{\omega}_x$	6.0000 deg/s
$\boldsymbol{\omega}_y$	0.1146 deg/s
$\boldsymbol{\omega}_z$	0.2865 deg/s

C. Nearly Flat HAMR SO in GTO

The second example application is a three-orbit propagation of a nearly flat, HAMR SO in GTO. Like the rocket body SO, the HAMR SO is modeled as a closed rectangular prism, but with side lengths 0.5, 0.25, and 0.001 m. The mass of the SO is 0.00475 kg, which gives the SO an area-to-mass ratio similar to that of Kapton, a substance commonly used to thermally insulate satellites [55]; the inertia parameters of the SO are given in Table 4a. No center-of-mass offset is assumed in the SO, and the coefficients of specular and diffuse reflection are taken to be 0.60 and 0.26, respectively, for all surfaces; these values are consistent with Kapton [55].

The force model consists of a 33 × 33 interpolated implementation of the geopotential, aerodynamic drag, SRP, and point-mass lunisolar gravitational forces [56]. For the 6DOF and hybrid models, the SRP force is calculated for each panel of the SO as described by Früh et al. [55]. As with aerodynamic drag, the SRP force for the 3DOF-only model is calculated using a single, constant area value based on an assumption of a spherical body [55].

The highly eccentric GTO necessitates a high-degree/order geopotential near periapsis, but a lower-degree/order field is acceptable near apoapsis. The interpolated gravity model requires

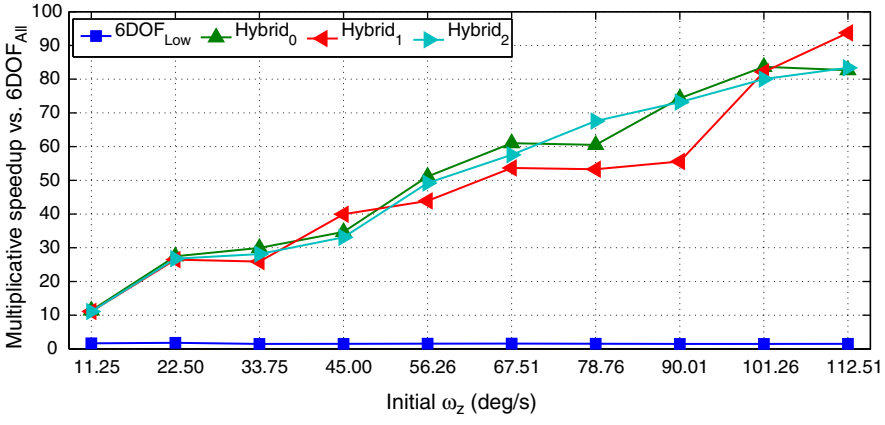

Fig. 6 Multiplicative speedups of hybrid and "Low" 6DOF propagations compared with "All" 6DOF propagation.

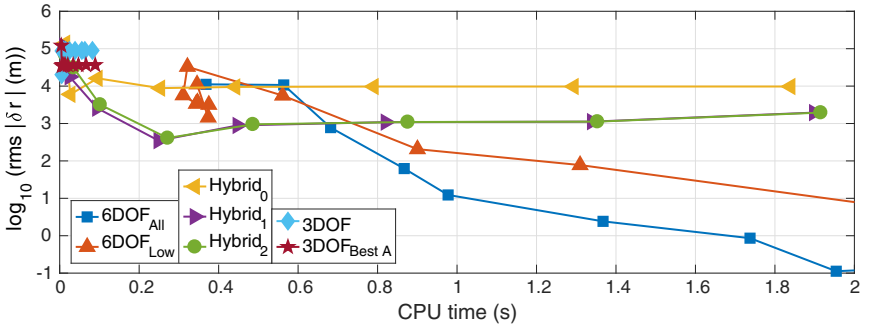

Fig. 7 RMS position error as a function of CPU time for three-orbit propagation of a HAMR SO in GTO.

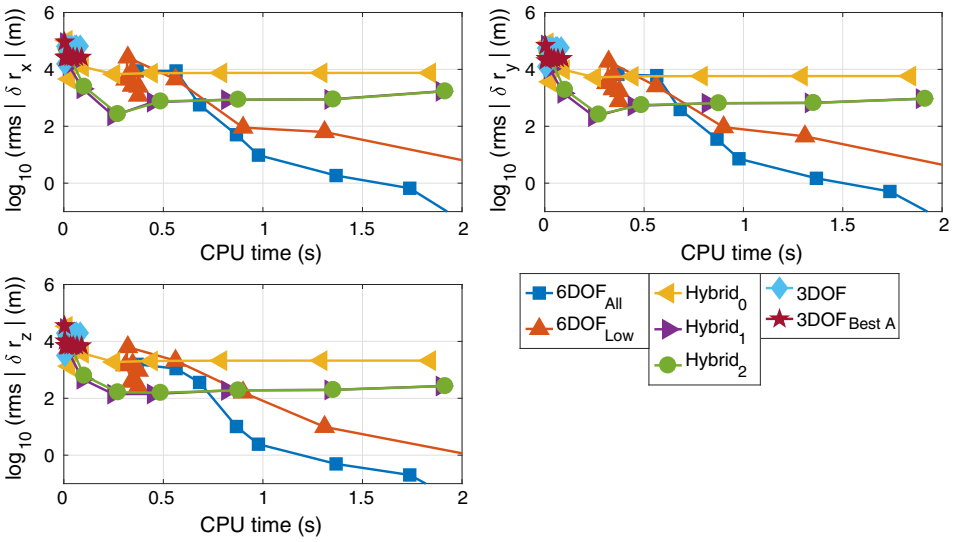

Fig. 8 ECI componentwise RMS position error as a function of CPU time for three-orbit propagation of a HAMR SO in GTO.

significantly less compute effort than the spherical harmonics formulation used in the LEO example, eliminating the need for a variable-degree/order model to obtain an efficient propagation.[‡‡] For 6DOF and hybrid propagations, torques caused by the gravity gradient and aerodynamic drag are considered. Torques due to SRP are neglected because, for a rectangular prism body with uniform reflectance properties, the net SRP torque is always zero under the current SRP model [57]. In the case of an asymmetrical SO, SRP torque is likely to be a significant driver of rotational motion due to the HAMR nature of the SO [55]. Selection of an alternative closed-form attitude solution that approximates the effects of SRP torques may be appropriate (e.g., Zanardi and de Moraes [23]).

The SO initial conditions are given in Tables 4b and 4c. The rotational state corresponds to a 1 revolution-per-minute rotation rate about the minimum inertia axis.

Simulation results are summarized in Figs. 7 and 8; the caption meanings are the same as for Figs. 3 and 4.[§§] Expectedly, the 3DOF propagations are again the most efficient, but the RMS error floors for the averaged area and the best-case area solutions are both greater than 20 km.[¶¶] The "Low" 6DOF propagation achieves an RMS error of approximately 1.45 km before the required CPU time begins to increase due to decreases in integration tolerance for the translational states. As in the rocket body example, a region is found in which the hybrid method provides improved accuracy compared with the 3DOF propagation and improved efficiency compared with the "Low" 6DOF propagation. The Hybrid_1 solution achieves an RMS error less than 10 km approximately three times faster than the "Low" 6DOF propagator and reaches sub-kilometer-level RMS position errors approximately 2.5 times faster than the "All" 6DOF solution. (The "All" solution is faster than the "Low" solution at this—and all tighter—accuracy levels.)

This simulation starkly shows the differences that can arise in the Hybrid_1 and Hybrid_2 solutions versus the Hybrid_0 solution. The additional variable transformations that differentiate Hybrid_1 from Hybrid_0 recover periodic solution terms related to averaging over the orbital period. Meanwhile, moving from Hybrid_1 to Hybrid_2 recovers periodic terms related to averaging over a body orientation angle. The amplitudes of the averaged variations related to the orbital period are generally the larger of the two by a significant margin, resulting in the observed trends [8]. It is therefore advisable to retain at least the Hybrid_1 solution, though, for the cases tested, any additional accuracy gained by using the Hybrid_2 solution is likely to be offset by the corresponding increase in CPU time.

For this example, the relative integration tolerance sweet spot for the hybrid method is approximately 10^{-6} to 10^{-9}, which is not as tight as that for the rocket body example. This result is due to 1) the increased importance of accurate attitude information for the accurate translational state prediction of the HAMR SO and 2) the decreased validity of the closed-form solution's assumption that gravity-gradient torque is the only torque acting on the SO. The approximations of the hybrid method are more detrimental for the HAMR SO than for the rocket body due to the rocket body's higher density and its spin axis.

[‡‡]The interpolated model could also be used for the LEO case. However, an example featuring the spherical harmonics formulation is included because of its ubiquity and to demonstrate the use of the hybrid method with dynamics models of various costs.

[§§]As in the rocket body example, the interested reader is directed to Refs. [8, 9, 54] for more information on the accuracy of the closed-form attitude solution.

[¶¶]The averaged area value is 0.04192 m^2, and the best-case area is 0.07258 m^2.

(Rotation about the maximum-inertia axis is likely to be more stable than rotation about the minimum-inertia axis because of energy dissipation effects [58].)

More generally, from the two numerical examples, it is seen that the most favorable tolerance level for the hybrid method corresponds to the "knee" in the error versus CPU time curve; the point at which the magnitude of the slope of the curve created by successively decreasing the integration tolerance begins to decrease.*** Unfortunately, the tolerance value for this point is dependent on not only the physical and dynamic properties of the simulation, but the ODE solver and the step size selection algorithm, as well. Further, in practice, the speed advantages of the hybrid method may be lost if a high-fidelity 6DOF reference solution must be generated repeatedly to determine the optimal tolerance for the hybrid method. It is therefore likely infeasible to pronounce a specific integration tolerance value range applicable to all scenarios.

This type of deficiency is not unique to the hybrid method. The loosest integration tolerance that reaches the accuracy floor of the 3DOF propagation is unlikely to be known a priori, potentially leading to significant computational waste if an overly tight tolerance is selected. Additionally, while the "Low"lara 6DOF method can provide improved efficiency compared with a full 6DOF propagation over a range of integration tolerances for the translational state, this range is also problem dependent. Even if full 6DOF propagation is used, there is no single integration tolerance that is optimal across all applications [59].

IV. Conclusions

The limiting assumptions—and, thus, limited accuracy—of 3DOF space object (SO) state prediction and the high computational burden of full 6DOF propagation leave room for intermediate techniques. In this work, one such option is developed: a semianalytical, hybrid special/GP algorithm in which the translational state is propagated numerically, informed by closed-form approximations of the rotational state. The hybrid method calculates body translational forces like aerodynamic drag and solar radiation pressure (SRP) using a dynamically updated attitude and a user-defined SO physical model. This force model contrasts with the typical assumption of a spherical body used by 3DOF propagations. At the same time, the hybrid method may take larger step sizes than a full 6DOF propagation because the attitude is not part of the numerically integrated state.

The hybrid method is agnostic to the choice of closed-form attitude solution, allowing a practitioner to select the algorithm that best fits their needs. The method is illustrated using a perturbation solution, derived using the Lie-Deprit method, and the capabilities of this implementation are demonstrated in two example simulations. Deviations from the assumptions of the perturbation solution are addressed by reinitializing the attitude solution procedure once per orbit revolution. The hybrid method is shown to produce position predictions more than an order of magnitude more accurate than a best-case 3DOF propagation at approximately one-third of the computational cost of a customized fully numerical 6DOF propagation. It is also demonstrated that efficiency gains realizable via the hybrid method increase as the rotation rate of the object increases because the numerical ODE solver does not have to directly propagate the fast-changing attitude states. However, as with any technique involving numerical integration, care must be taken in the selection of the integration tolerance (for a variable-step method) or step size (for a fixed-step method): If the tolerance is too loose, minimal improvement over a 3DOF propagation may be seen, while, if the tolerance is too tight, a full 6DOF propagation may produce more accurate results with greater efficiency.

At near-optimal integration tolerances, the hybrid method offers a bridge between 3DOF and fully numerical 6DOF propagations. The improved accuracy attained for SO position state prediction versus 3DOF cannonball propagation has the potential to, for example, decrease uncertainties in conjunction assessments. The approximate knowledge of space object attitude produced by the hybrid method may be important for applications such as active debris removal. At the same time, the speed increase versus full 6DOF propagation makes the hybrid method more amenable to large-catalog applications.

***This discussion assumes a variable-step ODE solver. In the case of a fixed-step method, the role of the integration tolerance is played by the step size.

Acknowledgments

This work was funded, in part, by a Phase II SBIR from the Air Force Research Laboratory, contract FA9453-14-C-0295, under a subcontract from Emergent Space Technologies, Inc. The authors would also like to gratefully acknowledge fruitful correspondence with Martin Lara.

References

[1] Fonte, D. J., Neta, B., Sabol, C., and Danielson, D. A., "Comparison of Orbit Propagators in the Research and Development Goddard Trajectory Determination System (R & D GTDS). Part I: Simulated Data," *AAS/AIAA Astrodynamics Specialist Conference*, AAS Paper 1995-431, Springfield, VA, Aug. 1995.

[2] Setty, S. J., Cefola, P. J., Montenbruck, O., Fiedler, H., and Lara, M., "Investigating the Suitability of Analytical and Semi-Analytical Satellite Theories for Space Object Catalogue Maintenance in Geosynchronous Regime," *AAS/AIAA Astrodynamics Specialist Conference*, AAS Paper 13-769, Springfield, VA, Aug. 2013.

[3] Früh, C., and Jah, M. K., "Attitude and Orbit Propagation of High Area-to-Mass Ratio (HAMR) Objects Using a Semi-Coupled Approach," *The Journal of the Astronautical Sciences*, Vol. 60, No. 1, 2013, pp. 32–50. doi:10.1007/s40295-014-0013-1

[4] Cefola, P. J., Long, A. C., and Holloway, G., Jr., "The Long-Term Prediction of Artificial Satellite Orbits," *AIAA 12th Aerospace Sciences Meeting*, AIAA Paper 1974-0170, 1974. doi:10.2514/6.1974-170

[5] Santoni, F., Cordelli, E., and Piergentili, F., "Determination of Disposed-Upper-Stage Attitude Motion by Ground-Based Optical Observations," *Journal of Spacecraft and Rockets*, Vol. 50, No. 3, 2013, pp. 701–708. doi:10.2514/1.A32372

[6] Ojakangas, G. W., Anz-Meador, P., and Cowardin, H., "Probable Rotation States of Rocket Bodies in Low Earth Orbit," *13th Annual Advanced Maui Optical and Space Conference*, Maui Economic Development Board, Maui, HI, 2012.

[7] Yanagisawa, T., and Kurosaki, H., "Shape and Motion Estimate of LEO Debris Using Light Curves," *Advances in Space Research*, Vol. 50, No. 1, 2012, pp. 136–145. doi:10.1016/j.asr.2012.03.021

[8] Lara, M., and Ferrer, S., "Closed Form Perturbation Solution of a Fast Rotating Triaxial Satellite Under Gravity-Gradient Torque," *Cosmic Research*, Vol. 51, No. 4, 2013, pp. 289–303. doi:10.1134/S0010952513040059

[9] Hatten, N., and Russell, R. P., "The Eccentric Case of a Fast-Rotating, Gravity-Gradient-Perturbed Satellite Attitude Solution," *27th AAS/AIAA Space Flight Mechanics Meeting*, AAS Paper 17-373, , Springfield, VA, Feb. 2017.

[10] Deprit, A., "Canonical Transformations Depending on a Small Parameter," *Celestial Mechanics*, Vol. 1, No. 1, 1969, pp. 12–30. doi:10.1007/BF01230629

[11] Nayfeh, A. H., *Perturbation Methods*, Wiley-VCH, Weinheim, Germany, 2000, pp. 1–2, 228–307.

[12] Awad, A., Narang-Siddarth, A., and Weisman, R., "The Method of Multiple Scales for Orbit Propagation with Atmospheric Drag," *AIAA Guidance, Navigation, and Control Conference*, AIAA Paper 2016-1370, 2016. doi:10.2514/6.2016-1370

[13] Glandorf, D. R., "Gravity Gradient Torque for an Arbitrary Potential Function," *Journal of Guidance, Control, and Dynamics*, Vol. 9, No. 1, 1986, pp. 122–124. doi:10.2514/3.20078

[14] Holland, R. L., and Sperling, H. J., "A First-Order Theory for the Rotational Motion of a Triaxial Rigid Body Orbiting an Oblate Primary," *The Astronomical Journal*, Vol. 74, No. 3, 1969, pp. 490–496. doi:10.1086/110826

[15] Heard, W. B., *Rigid Body Mechanics: Mathematics, Physics and Applications*, Wiley-VCH, Weinheim, Germany, 2006, pp. 88–145.

[16] Crenshaw, J. W., and Fitzpatrick, P. M., "Gravity Effects on the Rotational Motion of a Uniaxial Artificial Satellite," *AIAA Journal*, Vol. 6, No. 11, 1968, pp. 2140–2145. doi:10.2514/3.4946

[17] Hitzl, D. L., and Breakwell, J. V., "Resonant and Non-Resonant Gravity-Gradient Perturbations of a Tumbling Tri-Axial Satellite," *Celestial Mechanics*, Vol. 3, No. 3, 1971, pp. 346–383. doi:10.1007/BF01231806

[18] Cochran, J. E., "Effects of Gravity-Gradient Torque on the Rotational Motion of a Triaxial Satellite in a Precessing Elliptic Orbit," *Celestial Mechanics*, Vol. 6, No. 2, 1972, pp. 127–150. doi:10.1007/BF01227777

[19] Lara, M., Fukushima, T., and Ferrer, S., "First-Order Rotation Solution of an Oblate Rigid Body Under the Torque of a Perturber in Circular Orbit," *Astronomy and Astrophysics*, Vol. 519, Sept. 2010, pp. A1–10. doi:10.1051/0004-6361/200913880

[20] Lara, M., Fukushima, T., and Ferrer, S., "Ceres' Rotation Solution Under the Gravitational Torque of the Sun," *Monthly Notices of the Royal Astronomical Society*, Vol. 415, No. 1, 2011, pp. 461–469. doi:10.1111/mnr.2011.415.issue-1

[21] San-Juan, J. F., Lopez, L. M., and Lopez, R., "Higher-Order Analytical Attitude Propagation of an Oblate Rigid Body Under Gravity-Gradient Torque," *Mathematical Problems in Engineering*, Vol. 2012, 2012, pp. 1–15. doi:10.1155/2012/123138

[22] Van der Ha, J. C., "Perturbation Solution of Attitude Motion Under Body-Fixed Torques," *Acta Astronautica*, Vol. 12, No. 10, 1985, pp. 861–869. doi:10.1016/0094-5765(85)90103-1

[23] Zanardi, M. C., and Vilhena de Moraes, R., "Analytical and Semi-Analytical Analysis of an Artificial Satellite's Rotational Motion," *Celestial Mechanics and Dynamical Astronomy*, Vol. 75, No. 4, 2000, pp. 227–250. doi:10.1023/A:1008358801859

[24] Zanardi, M. C., Quirelli, I. M. P., and Kuga, H. K., "Analytical Attitude Prediction of Spin Stabilized Spacecrafts Perturbed by Magnetic Residual Torque," *Advances in Space Research*, Vol. 36, No. 3, 2005, pp. 460–465. doi:10.1016/j.asr.2005.07.020

[25] Zanardi, M. C., and Moreira, L. S., "Analytical Attitude Propagation with Non-Singular Variables and Gravity Gradient Torque for Spin Stabilized Satellite," *Advances in Space Research*, Vol. 40, No. 1, 2007, pp. 11–17. doi:10.1016/j.asr.2007.04.047

[26] Bois, E., and Kovalevsky, J., "Analytical Model of the Rotation of an Artificial Satellite," *Journal of Guidance, Control, and Dynamics*, Vol. 13, No. 4, 1990, pp. 638–643. doi:10.2514/3.25381

[27] Bois, E., "First-Order Theory of Satellite Attitude Motion Application to Hipparcos," *Celestial Mechanics*, Vol. 39, No. 4, 1986, pp. 309–327. doi:10.1007/BF01230479

[28] Bois, E., "Second-Order Theory of the Rotation of an Artificial Satellite," *Celestial Mechanics*, Vol. 42, Nos. 1–4, 1988, pp. 141–168. doi:10.1007/BF01232953

[29] Ferrandiz, J. M., and Sansaturio, M. E., "Elimination of the Nodes When the Satellite is a Non Spherical Rigid Body," *Celestial Mechanics and Dynamical Astronomy*, Vol. 46, No. 4, 1989, pp. 307–320. doi:10.1007/BF00051485

[30] Ferrandiz, J. M., Sansaturio, M. E., and Caballero, R., "On the Roto-Translatory Motion of a Satellite of an Oblate Primary," *Celestial Mechanics and Dynamical Astronomy*, Vol. 57, Nos. 1–2, 1993, pp. 189–202. doi:10.1007/BF00692473

[31] Ferrer, S., and Lara, M., "On Roto-Translatory Motion, Reductions and Radial Intermediaries," *Journal of the Astronautical Sciences*, Vol. 139, No. 1, 2011, pp. 21–39. doi:10.1007/s40295-013-0004-7

[32] Mohmmed, H. M., Ahmed, M. K., Owis, A., and Dwidar, H., "Analytical Solution of the Perturbed Orbit-Attitude Motion of a Charged Spacecraft in the Geomagnetic Field," *International Journal of Advanced Computer Science and Applications*, Vol. 4, No. 3, 2013, pp. 272–286. doi:10.14569/IJACSA.2013.040341

[33] Battin, R. H., *An Introduction to the Mathematics and Methods of Astrodynamics*, Rev. ed., AIAA, Reston, VA, 1999, pp. 447–450.

[34] Woodburn, J., and Tanygin, S., "Efficient Numerical Integration of Coupled Orbit and Attitude Trajectories Using an Encke Type Correction Algorithm," *AAS/AIAA Astrodynamics Specialist Conference*, AAS Paper 01-428, Springfield, VA, July–Aug. 2001.

[35] Le Fevre, C., Morand, V., Delpech, M., Gazzino, C., and Henriquel, Y., "Integration of Coupled Orbit and Attitude Dynamics and Impact on Orbital Evolution of Space Debris," *AAS/AIAA Space Flight Mechanics Meeting*, AAS Paper 15-335, Springfield, VA, Jan. 2015.

[36] Celletti, A., *Stability and Chaos in Celestial Mechanics*, Springer-Praxis, Berlin, 2006, pp. 83–88.

[37] Fukushima, T., "New Canonical Variables for Orbital and Rotational Motions," *Celestial Mechanics and Dynamical Astronomy*, Vol. 60, No. 1, 1994, pp. 57–68. doi:10.1007/BF00693092

[38] Fukushima, T., and Ishizaki, H., "Numerical Computation of Incomplete Elliptic Integrals of a General Form," *Celestial Mechanics and Dynamical Astronomy*, Vol. 59, No. 3, 1994, pp. 237–251. doi:10.1007/BF00692874

[39] Fukushima, T., "Precise and Fast Computation of a General Incomplete Elliptic Integral of Third Kind by Half and Double Argument Transformations," *Journal of Computational and Applied Mathematics*, Vol. 236, No. 7, 2012, pp. 1961–1975. doi:10.1016/j.cam.2011.11.007

[40] Fukushima, T., "Fast Computation of a General Complete Elliptic Integral of Third Kind by Half and Double Argument Transformations," *Journal of Computational and Applied Mathematics*, Vol. 253, Dec. 2013, pp. 142–157. doi: 10.1016/j.cam.2013.04.015

[41] Fukushima, T., "Precise and Fast Computation of Jacobian Elliptic Functions by Conditional Duplication," *Numerische Mathematik*, Vol. 123, No. 4, 2013, pp. 585–605. doi: 10.1007/s00211-012-0498-0

[42] Fukushima, T., "Personal ResearchGate Web Page," 2014, https://www.researchgate.net/profile/Toshio_Fukushima [accessed Aug. 2014].

[43] Radhakrishnan, K., and Hindmarsh, A., "Description and use of LSODE, the Livermore Solver for Ordinary Differential Equations," Lawrence Livermore National Lab. TR UCRL-ID-113855, Livermore, CA, 1993.

[44] Fukushima, T., "Simple, Regular, and Efficient Numerical Integration of Rotational Motion," *The Astronomical Journal*, Vol. 135, No. 6, 2008, pp. 2298–2322. doi:10.1088/0004-6256/135/6/2298

[45] Lara, M., "Short-Axis-Mode Rotation of a Free Rigid Body by Perturbation Series," *Celestial Mechanics and Dynamical Astronomy*, Vol. 118, No. 3, March 2014, pp. 221–234. doi:10.1007/s10569-014-9532-0

[46] Lara, M., "Short-Axis-Mode Rotation in Complex Variables," *Proceedings of the Journées des Systèmes de Référence et de al Rotation Terrestre*, Alicante, Spain, Sept. 2017, https://web.ua.es/journees2017/abstracts.html.

[47] United Launch Alliance, *Atlas V Launch Services User's Guide*, United Launch Alliance, Centennial, CO, March 2010.

[48] NASA, "NASA Space Science Data Coordinated Archive," 2016, http://nssdc.gsfc.nasa.gov/nmc/masterCatalog.do?sc=2009-041B [accessed June 2016].

[49] De Pontieu, B., "Database of Photometric Periods of Artificial Satellites," *Advances in Space Research*, Vol. 19, No. 2, 1997, pp. 229–232. doi:10.1016/S0273-1177(97)00005-7

[50] McCants, M., "Mike McCants' BWGS PPAS Page," 2016, https://www.prismnet.com/mmccants/bwgs/index.html [accessed June 2016].

[51] Hatten, N., and Russell, R. P., "A Smooth and Robust Harris-Priester Atmospheric Density Model," *26th AAS/AIAA Space Flight Mechanics Meeting*, AAS Paper 16-406, Springfield, VA, Feb. 2016.

[52] Hatten, N., and Russell, R. P., "A Smooth and Robust Harris-Priester Atmospheric Density Model for Low Earth Orbit Applications," *Advances in Space Research*, Vol. 59, No. 2, 2017, pp. 571–586. doi:10.1016/j.asr.2016.10.015

[53] Doornbos, E., "Thermospheric Density and Wind Determination from Satellite Dynamics," Ph.D. Dissertation, TU Delft, Delft, The Netherlands, 2011.

[54] Hatten, N., "Space Object Translational and Rotational State Prediction and Sensitivity Calculation," Ph.D. Dissertation, The Univ. of Texas at Austin, Austin, TX, Dec. 2016.

[55] Früh, C., Kelecy, T. M., and Jah, M. K., "Coupled Orbit-Attitude Dynamics of High Area-to-Mass Ratio (HAMR) Objects: Influence of Solar Radiation Pressure, Earth's Shadow and the Visibility in Light Curves," *Celestial Mechanics and Dynamical Astronomy*, Vol. 117, No. 4, 2013, pp. 385–404. doi:10.1007/s10569-013-9516-5

[56] Arora, N., Vittaldev, V., and Russell, R. P., "Parallel Computation of Trajectories Using Graphics Processing Units and Interpolated Gravity Models," *Journal of Guidance, Control, and Dynamics*, Vol. 38, No. 8, 2015, pp. 1345–1355. doi:10.2514/1.G000571

[57] Wetterer, C. J., Crassidis, J. L., Linares, R., Kelecy, T. M., Ziebart, M. K., Jah, M. K., and Cefola, P. J., "Refining Space Object Radiation Pressure Modeling with Bidirectional Reflectance Distribution Functions," *Journal of Guidance, Control, and Dynamics*, Vol. 37, No. 1, 2014, pp. 185–196.
doi:10.2514/1.60577

[58] Kaplan, M. H., *Modern Spacecraft Dynamics and Control*, Wiley, New York, 1976, pp. 61–64.

[59] Urrutxua, H., Bombardelli, C., Roa, J., and Gonzalo, J. L., "Quantification of the Performance of Numerical Orbit Propagators," *26th AAS/AIAA Space Flight Mechanics Meeting*, AAS Paper 16-351, Springfield, VA, Feb. 2016.